ELECTRON DIFFRACTION INVESTIGATION OF CRYSTALLOGRAPHIC TEXTURE OF THIN FILMS

LI TANG*, SHANLIN DUAN*, and DAVID E. LAUGHLIN**

*IBM, Storage Systems Division, 5600 Cottle Road, N76/050, San Jose, CA 95193
** Data Storage Systems Center and Department of Materials Science and Engineering, Carnegie Mellon University, Pittsburgh, PA 15213

ABSTRACT

A method of investigating thin film crystallographic texture by electron diffraction is reviewed. The reciprocal lattices of fibrous and lamellar textured thin films are spherical belts around the texture axis. Equations describing the projection of the spherical belts onto the Ewald sphere along the texture axis direction are presented. Based on these equations the geometric and intensity evolution of the electron diffraction patterns with the tilt angle about an arbitrary axis in the film plane can be analyzed in a systematic way. The geometric characteristics of the electron diffraction patterns are then used to derive the texture axis directional index and its angular distribution. The way to determine the equal-intensity circular arcs on the diffraction pattern is also discussed. This method can be applied to both single layered and multilayered thin films of various applications.

1. Introduction

The orientations of grains in polycrystalline thin films usually have a preferred orientation. This preferred orientation can be either a crystallographic direction *[uvw]*, i.e. fibrous texture, or a reciprocal lattice direction *[hkl]**, i.e. lamellar texture, which is the normal direction to *(hkl)* planes in real space. For thin films the reference direction is usually the normal direction to the substrate surface. In this paper we review a method of investigating thin film fibrous and lamellar texture by electron diffraction. Both the geometric and intensity characteristics of electron diffraction patterns of the textured thin films will be discussed.

Mat. Res. Soc. Symp. Proc. Vol. 562 ©1999 Materials Research Society

2. Reciprocal Lattice of Fibrous and Lamellar Textured Thin films

This section presents a unified method of constructing and indexing the reciprocal space of fibrous and lamellar textured thin films [1]. We assume that the texture axis $\boldsymbol{R}=u\boldsymbol{a}+v\boldsymbol{b}+w\boldsymbol{c}$ $=[uvw]$ or $\boldsymbol{G}_{h'k'l'} = h'\boldsymbol{a}^*+k'\boldsymbol{b}^*+l'\boldsymbol{c}^* = [h'k'l']^*$ is distributed within an angle of α. For an $\{hkl\}$ family with a multiplicity factor of P there are N reciprocal spherical belts around the texture axis on the $\{hkl\}$ reciprocal sphere with a radius of $G_{\{hkl\}} = 1/d_{hkl}$, where N is the number of distinct angles between the $\{hkl\}$ plane normal and the texture axis direction. These N reciprocal spherical belts can be indexed as hkl_i, $i = 0, 1, 2, 3 .. N-1$ for $\{hkl\}$ having at least one plane $90°$ to the texture axis *and* $i = 1, 2, 3, .. N$ for $\{hkl\}$ that has no planes $90°$ to the texture axis. Here, i is in the order of decreasing angle values ρ_i (Fig. 1), which can be calculated by

$$\cos \rho_i = \boldsymbol{R}_{uvw} \bullet \boldsymbol{G}_{\{hkl\}i}/RG_{\{hkl\}} = (h_i u+k_i v+l_i w)/ RG_{\{hkl\}}= n_i/RG_{\{hkl\}} \qquad (1a)$$

for a fibrous texture (where n_i is an integer) and

$$\cos \rho_i = \boldsymbol{G}_{h'k'l'} \bullet \boldsymbol{G}_{\{hkl\}i}/(G_{h'k'l'}G_{\{hkl\}}) = (h_i u'+k_i v'+l_i w')/(G_{h'k'l'}G_{\{hkl\}}) \qquad (1b)$$

for a lamellar texture, where $u'\boldsymbol{a}+v'\boldsymbol{b}+w'\boldsymbol{c} = h'\boldsymbol{a}^*+k'\boldsymbol{b}^*+l'\boldsymbol{c}^*$.

The *ith* reciprocal belt consists of P_i of $\{hkl\}$ planes. It is obvious that

$$P = \sum_{i=0 \text{ or } 1}^{N-1 \text{ or } N} P_i \qquad (2)$$

and $N \le M \le P$, $P_i \ge p_i$, where M is the maximum possible number of distinct angles between $[uvw]$ *or* $[h'k'l]^*$ and $\{hkl\}$ planes, p_i is the minimum number of planes in $\{hkl\}$ being in the *ith* spherical belt. Tables 1 and 2 summarize M and p_i between any given $[uvw]$ and/or $[h'k'l']^*$ and an $\{hkl\}$ family of planes for cubic and hexagonal systems, respectively [1,2]. In Tables 1 and 2, the order for the p_i is from N *or* $N-1$ to 1 *or* 0 and for n $(n \ge 2)$ consecutive spherical belts having the same p_i it is written as p_i x n. In addition, a p_i with an asterisk indicates the planes are 90° from the texture axis.

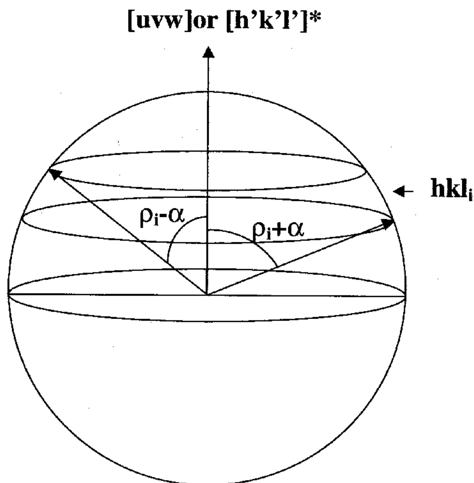

Fig. 1. The hkl_i reciprocal spherical belt of an *{hkl}* for a *[uvw]* or *[h'k'l']** textured film.

Table 1. Maximum number of distinct angles between any given direction/plane and all the faces of a given plane family in cubic system and the p_i

Direction	[uvw]	[uuw]	[0vw]	[110]	[111]	[001]
Plane	[hkl]*	[hhl]*	[0kl]*	[110]*	[111]*	[001]*
{hkl }(24)	24(1x24)	12(2x12)	12(2x12)	6(4x6)	4(6x4)	3(8x3)
{hhl}(12)	12(1x12)	7(1,2x5,1)	6(2x6)	4(4,2,4,2*)	3(3,6,3)	2(4,8)
{0kl }(12)	12(1x12)	6(2x6)	8(1x2,2x4,1x2)	4(2,4x2,2)	2(6x2)	3(4x2,4*)
{0kk}(6)	6(1x6)	4(2,1,2,1*)	4(1,2x2,1)	3(1,4,1*)	2(3,3*)	2(4,2*)
{hhh}(4)	4(1x4)	3(1,2,1)	2(2x2)	2(2,2*)	2(1,3)	1(4)
{001}(3)	3(1x3)	2(1,2)	3(1x2,1*)	2(2,1*)	1(3)	2(1,2*)

Table 2. Maximum number of distinct angles between any given direction/plane and all the faces of a given plane family in hexagonal system and the p_i

Direction	[uv.w]	[uu.w]	[0v.w]	[uv.0]	[11.0]	[01.0]	[00.1]
Plane	[hk.l]*	[hh.l]*	[0k.l]*	[hk.0]*	[11.0]*	[01.0]*	[00.1]*
{hk.l}(12)	12(1x12)	6(2x6)	6(2x6)	6(2x6)	3(4x3)	3(4x3)	1(12)
{hh.l} (6)	6(1x6)	4(1,2x2,1)	3(2x3)	3(2x3)	2(2,4)	2(4,2*)	1 (6)
{0kl } (6)	6(1x6)	3(2x3)	4(1,2,1,2)	3(2x3)	2(4,2*)	2(2,4)	1(6)
{hk.0}(6)	6(1x6)	3(2x3)	3(2x3)	6(1x6)	3(2x3)	3(2x3)	1(6*)
{hh.0}(3)	3(1x3)	2(1,2)	2(2,1*)	3(1x3)	2(1,2)	2(2,1*)	1(3*)
{0k.0}(3)	3(1x3)	2(2,1*)	2(1,2)	3(1x3)	2(2,1*)	2(1,2)	1(3*)
{00.1}(1)	1(1)	1(1)	1(1)	1(1*)	1(1*)	1(1*)	1(1)

3. Evolution of the Electron Diffraction Pattern with Tilt Angle

For polycrystalline thin films electron scattering can be regarded as kinematical [3]. For an incident electron beam with a wavelength of λ, the integrated diffraction intensity on the Ewald sphere for the *ith* reciprocal belt can be written as:

$$\frac{I_{hkli}}{I_0} \propto \lambda^2 D_i P_i \left(\frac{F_{hkl}}{V_c}\right)^2 \int \frac{\sin^2 \pi t s}{(\pi s)^2} dA(s) \tag{3}$$

where I_0 is the incident electron beam intensity, F_{hkl} the structure factor for *{hkl}*, V_c the volume of the unit cell, t the film thickness, s the deviation parameter along the film thickness direction which we also assume to be the texture axis direction, D_i the number of grains per unit area for the *ith* spherical belt, *dA(s)* is the area element. For the *ith* spherical belt:

$$D_i = \frac{n}{4\pi G_{hkl}^2 \sin\alpha \sin\rho_i} \tag{4}$$

where n is the total number of grains, which are identical and uniformly distributed. We define in Figure 2 the coordinate system and parameters needed to determine $dA(s)$. In Fig. 2 the incident electron beam direction is along the z axis, the tilt axis in the film plane is along x axis, the Ewald sphere is the x-y plane ($s = 0$), ON is the texture axis direction, its projection along z axis on the x-y plane is the y axis, β is the tilt angle. From Fig. 2 the following can be derived:

$$s = G_{hkl} \sin\theta / \cos\beta, \ s_z = s \cos\beta \quad \pi/2 \geq \theta \geq -\pi/2 \tag{5a}$$

$$dA(s) = \omega(s)\, G_{hkl}^2 \cos\theta \, d\theta = \omega(s)\, G_{hkl} \cos\beta \, ds \tag{5b}$$

where $\omega(s)$ is the angle subtended by the circular arc which is the intersection of the spherical belt with the circle of radius of $G_{hkl}\cos\theta$ at $z = s_z$. It should be pointed out that all points on this circle have the same s value given the tilt angle β.

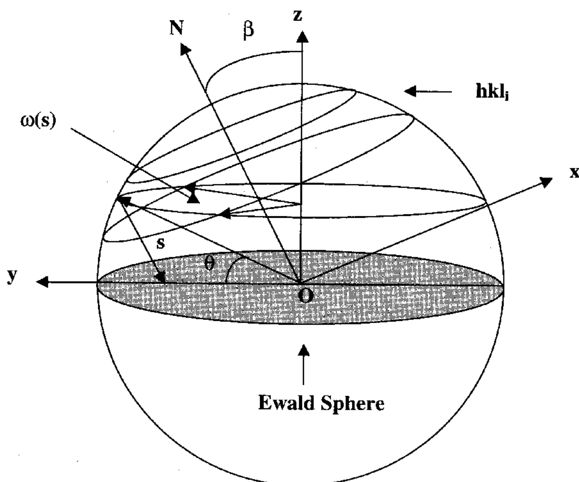

Figure 2. The hkl_i reciprocal belt of an $\{hkl\}$ after the texture axis is tilted about the x axis from the incident electron beam direction (i.e. z axis).

The integrated electron diffraction intensity from the *ith* spherical belt is distributed on the Ewald sphere in a region defined by the projection of the spherical belt along the film thickness direction, i.e. texture axis direction in this discussion. This projection is an elliptic band bounded by the following ellipses (Fig. 3):

$$\frac{x^2}{(G_{hkl}\sin(\rho_i+\alpha))^2}+\frac{y^2}{(G_{hkl}\sin(\rho_i+\alpha)/\cos\beta)^2}=1$$

(6a)

$$\frac{x^2}{(G_{hkl}\sin(\rho_i-\alpha))^2}+\frac{y^2}{(G_{hkl}\sin(\rho_i-\alpha)/\cos\beta)^2}=1$$

(6b).

On the other hand the projection of the constant s circle of radius $G_{hkl}cos\theta$ (also see Fig. 2, the portion of this circle intersected with the spherical belt diffracts with the same intensity for a given tilt angle β) along the texture axis on the x-y plane is an off-center circle:

$$x^2+(y+G_{hkl}\sin\theta tg\beta)^2=(G_{hkl}\cos\theta)^2$$
$$\pi/2\geq 6\geq -\pi/2$$

(7).

For the $s = 0$ circle where the Bragg law is exactly satisfied, its position is independent of the tilt angle β. In fact it is the circle defined by the intersection of the Ewald sphere with the reciprocal sphere of *{hkl}*. The $s = 0$ circle is also the *hkl* diffraction ring for thick and non-textured films. The intersection of the constant s circle with the elliptic band described by Eq. (6) is constant intensity circular arcs (see Fig. 3). In addition, the $\omega(s)$ at given θ and β is the angle subtended by the circular arcs, which can also be determined by the solution of Eqs. (7), (6a), and (6b).

We now apply Eqs. (3)-(7) to some special cases.

i. Case for which $\beta = 0$

When the texture axis is parallel to the incident electron beam,

$s = s_z = G_{hkl}\sin\theta$, *and* $\omega(s) = 2\pi \quad \pi/2-(\rho_i-\alpha) \geq \theta \geq \pi/2-(\rho_i+\alpha)$.

The diffraction intensity now distributes on the *x*-*y* plane in a circular band with $G_{hkl}\sin(\rho_i+\alpha) \geq R \geq G_{hkl}\sin(\rho_i-\alpha)$. Any circle in this circular band now is a constant intensity circle. The integrated intensity for the *ith* spherical belt is:

$$\left(\frac{I_{hkli}}{I_0}\right)_{\beta=0} \propto \frac{\lambda^2 n P_i}{2\sin\alpha\sin\rho_i G_{hkl}}\left(\frac{F_{hkl}}{V_c}\right)^2 \int_{G_{hkl}\cos(\rho_i+\alpha)}^{G_{hkl}\cos(\rho_i-\alpha)} \frac{\sin^2 \pi t s}{(\pi s)^2} ds \quad (8).$$

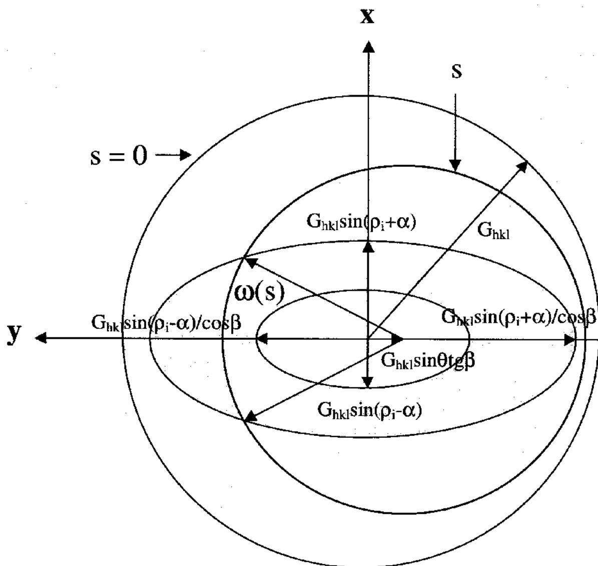

Figure 3. Projection of the *ith* reciprocal belt along the film thickness direction on the Ewald sphere and the equal intensity circular arc $\omega(s)$.

For $\rho_i = \pi/2$ and $s = 0$ circle which has a radius of G_{hkl}, the radius of the corresponding diffraction hkl_0 ring r_{hkl} on the screen is related to $G_{hkl} = 1/d_{hkl}$ by

$$L\lambda = r_{hkl}/G_{hkl} \tag{9}$$

where $L\lambda$ is the camera constant. Also the indices of the texture axis direction can be determined using following conditions:

$$hu + kv + lw = 0 \quad \text{for fibrous texture} \tag{10a}$$

$$hu' + kv' + lw' = 0 \quad \text{for lamellar texture} \tag{10b}$$

It should be noted that at least three hkl_0 rings are needed to determine $[uvw]$ or $[u'v'w'] = [hkl]^*$ by Eq. (10). For a lamellar texture it is often the case that there are no (hkl) planes satisfying Eq. (10b).

ii. Case for which $\rho_i = \pi/2$

From Eqs. (6) and (7) we have:

$$\omega_{hkl_0}(0) = 2\pi \qquad \beta < \alpha$$

$$\sin(\omega_{hkl_0}(0)) = \sin\alpha/\sin\beta \qquad \beta > \alpha \tag{11}$$

and the $\omega_{hkl_0}(0)$ is bisected by the tilt axis **OT** as shown in Figs. 4a and 4b. Thus the distribution angle α could be determined by the measured $\omega_{hkl_0}(0)$ from the diffraction pattern at given β and Eq. (11).

iii. Case for which $\rho_i \neq \pi/2$

Similarly for any hkl_i spherical belt we have

$$\omega_{hkl_i}(0) = 0 \qquad \beta < \pi/2-(\rho_i+\alpha) \tag{12a}$$

$$\cos(\omega_{hkl_i}(0)/2) = \cos(\rho_i+\alpha)/\sin\beta \qquad \pi/2-(\rho_i-\alpha) > \beta > \pi/2-(\rho_i+\alpha) \tag{12b}$$

$$\omega_{hkl_i}(0) = \cos^{-1}(\cos(\rho_i+\alpha)/\sin\beta) - \cos^{-1}(\cos(\rho_i-\alpha)/\sin\beta) \qquad \beta > \pi/2-(\rho_i-\alpha) \qquad (12c).$$

The arc described by Eq. (12b) is bisected by y axis (Fig. 5a). Eq. (12c) defines two arcs symmetric about y axis (Fig. 5b). The angle δ_i between the center point of the two arcs and y axis can be determined by:

$$\cos(\delta_i) = \cos(\rho_i)/\sin\beta \qquad \beta > \pi/2-(\rho_i-\alpha) \qquad (12d).$$

From Eqs. (12b), (12c), and (12d) we can also determine α and texture axis indices experimentally.

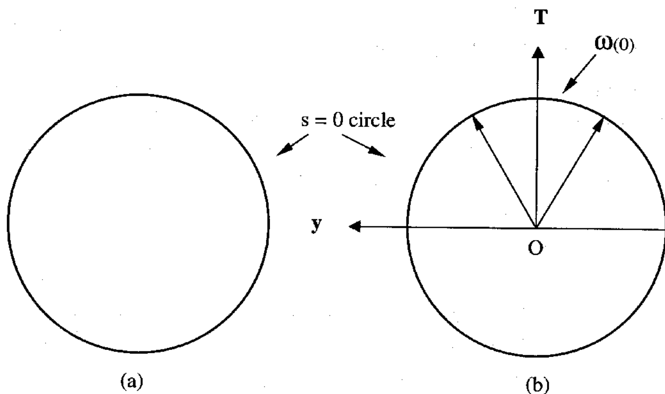

Figure 4. (a) hkl_0 $s = 0$ ring, $\beta < \alpha$, (b) hkl_0 $s = 0$ arc, $\beta > \alpha$.

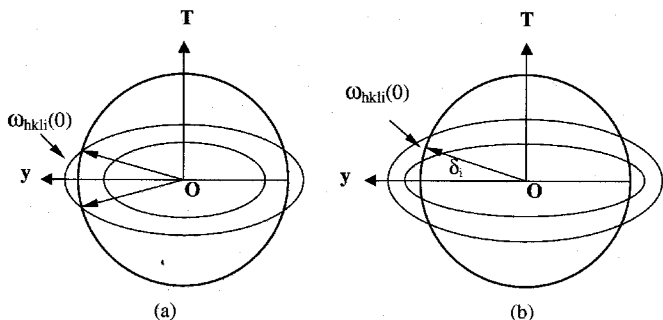

Figure 5. (a) hkl_i $s = 0$ arc , $\pi/2-(\rho_i-\alpha) > \beta > \pi/2-(\rho_i+\alpha)$, (b) hkl_i $s = 0$ arc , $\beta > \pi/2-(\rho_i-\alpha)$.

4. [011] textured Ta and (10 $\bar{1}$1)CoCrTa/(011)Cr

This section presents diffraction patterns of a *[011]* fibrous textured thin film (for cubic systems there is no need to distinguish fibrous and lamellar texture since *[hkl]//[hkl]**) of *bcc* Ta (*a = 0.303 nm*) [4,5] and a CoCrTa/Cr bi-layer film, where the CoCrTa (*hcp, a = 0.2507 nm, c = 0.4070 nm*) is (10 $\bar{1}$1) lamellar textured and the Cr (*bcc*, a = 0.2885 nm) is *(011)* textured [5, 6]. The *100 nm* thick *[011]* Ta film is sputter deposited on a glass substrate at *550 C°*. Figures 6a and 6b are the diffraction patterns of the *[011]* textured Ta film at *0°* and *54°* tilt. Fig. 6b indicates that this film also has some randomly oriented grains. Our on going research is to use dark field images taken from the diffraction ring due to randomly oriented grains and that from the diffraction arcs due to textured grains to deduce the percentage of gains having certain type of texture. From Fig. 6b the distribution angle α for the *[011]* textured axis is determined to be *10°* using Eqs. (11) and (12). The CoCrTa(*40 nm*)/Cr(*100 nm*) bilayer film is also sputter deposited on a glass substrate but at *150 C°*. Figure 7 is the diffraction pattern of the *(10 $\bar{1}\bar{1}$)*CoCrTa/Cr*(011)* bilayer film at *50°* tilt. Both of the *[10 $\bar{1}\bar{1}$]** and *[011]* texture axis have a distribution angle of *6°*. We also applied this

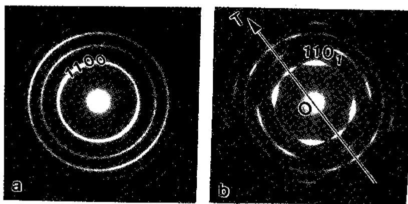

Fig. 6. Electron diffraction patterns of a [011] textured bcc Ta film at (a) *0°* and (b) *54°* tilt.

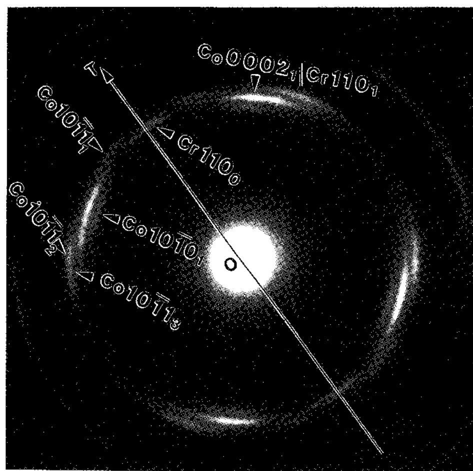

Fig. 7. Electron diffraction pattern of a (10 $\bar{1}$1)CoCrTa (*hcp*)/(011)Cr(*bcc*) bilayer film at *50°* tilt.

technique to crystallographic texture study of CoCrPt/Cr bi-layer films which have been used as media for longitudinal magnetic recording [7] and FeMn/NiFe/Co/Cu/Co/NiFe/Ta/Si spin valve multilayer films which have been used as high density magnetic recording read elements [8].

5. Summary

We have reviewed a method of investigating thin film crystallographic texture by electron diffraction. The approach is based on a detailed analysis of intensity weighted reciprocal space and its projection along the texture axis onto the Ewald sphere. Examples of *[011]* textured Ta and CoCrTa $[10\ \bar{1}1]^*$/Cr*[011]* have been presented. The concept of equal intensity circular arcs has been introduced which will be useful for electron diffraction pattern analysis of very thin films.

Acknowledgments

The authors are grateful to Weiming Lee and Yan Liu of IBM for their many useful suggestions. This work is supported in part by the National Science Foundation under grant *ECD-8907068* and an IBM Partnership Award (DEL).

References

1. L. Tang and D.E. Laughlin, J. Appl. Cryst. **29**, p.411 (1996).
2. B. Lu, L. Tang, D.N. Lambeth, and D.E. Laughlin, Proc. International Conference on Grain Growth, Ed. A. Weiland, B. Adams, and A. Rollet, TMS, Warrendole, PA, p. 529 (1998).
3. B.K. Vainshtein, *Structure Analysis by Electron Diffraction*, Pergamon, New York, 1964, p.70.
4. M.H. Read and C. Altman, Appl. Phys. Lett. **7**, p.51 (1965).
5. L. Tang, Y.C. Feng, L.L. Lee, and D.E. Laughlin, J. Appl. Cryst. **29**, p.419 (1996).
6. D.E. Laughlin, L. Tang, L.L. Lee, Y.N. Hsu, and D.N. Lambeth, Mat. Res. Soc. Symp. Proc., **475**, p.107 (1997).
7. L. Tang, D.E. Laughlin, D.N. Lambeth, and M.F. Doerner, J. Appl. Phys. **79**, p.5348 (1996).
8. L. Tang, D.E. Laughlin, and S. Gangopadhyay, J. Appl. Phys. **81**, p.4906 (1997).